

18. H. E. Garcia, R. A. Locarnini, T. P. Boyer, J. I. Antonov, in *World Ocean Atlas 2005, Vol. 3: Dissolved Oxygen, Apparent Oxygen Utilization, and Oxygen Saturation*, S. Levitus, Ed. (National Oceanic and Atmospheric Administration Atlas National Environmental Satellite, Data, and Information Service 63, U.S. Government Printing Office, Washington, DC, 2006), p. 1–342.
19. R. Schlitzer, <http://odv.awi.de> (2007).
20. HydroBase (13) quality-controlled data augmented with recent repeat transects and available Argo float profiles within the areas shown (Fig. 1) were objectively mapped using correlation scales of 1 year and 50 m. To ameliorate potential spatial bias due to recent sparser sampling, the meridional conductivity temperature depth and bottle sections used after 2000 were longitudinally centered within each area. Inspection of data distributions suggests that reported trends are not based on geographical shifts of data locations inside the investigation areas or seasonal shifts as a function of time, except as noted in the text.
21. Suspect data for 1989 were removed from Fig. 2D (offset from the surface to 1000 m), for 1963 from Fig. 2E (stations only in the southern part of the box), and for 1986 from Fig. 2F (oxygen increased from 400 m to a maximum at 1000 m).
22. Linear trends and their 95% confidence intervals were estimated as in (23), using annual 300- to 700-m averages of the objectively mapped fields. Degrees of freedom for the confidence intervals were determined from integral time scales as in (24).
23. C. Wunsch, *The Ocean Circulation Inverse Problem* (Cambridge Univ. Press, Cambridge, 1996).
24. H. von Storch, F. W. Zwiers, *Statistical Analysis in Climate Research* (Cambridge Univ. Press, Cambridge, 1999).
25. The Deutsche Forschungsgemeinschaft provided support as part of the German project Sonderforschungsbereich 754 (L.S.). Additional support was provided through the National Oceanic and Atmospheric Administration (NOAA) Office of Oceanic and Atmospheric Research (G.C.J.) and NSF award no. 0223869 (J.S.). Findings and conclusions in this article are those of the authors and do not necessarily represent the views of NOAA. Float data are collected and made freely available by the international Argo Project and contributing national programs (www.argo.ucsd.edu).

6 December 2007; accepted 20 March 2008
10.1126/science.1153847

A General Model for Food Web Structure

Stefano Allesina,^{1,2*} David Alonso,^{1,3} Mercedes Pascual^{1,4}

A central problem in ecology is determining the processes that shape the complex networks known as food webs formed by species and their feeding relationships. The topology of these networks is a major determinant of ecosystems' dynamics and is ultimately responsible for their responses to human impacts. Several simple models have been proposed for the intricate food webs observed in nature. We show that the three main models proposed so far fail to fully replicate the empirical data, and we develop a likelihood-based approach for the direct comparison of alternative models based on the full structure of the network. Results drive a new model that is able to generate all the empirical data sets and to do so with the highest likelihood.

Food webs (1–3) are paradigmatic examples of complex systems in nature (4). Despite the challenge posed by the intricacy of these trophic networks, simple models have been proposed for their topology that successfully capture a number of structural properties (5–7). These models have been influential in showing that the topology of food webs in nature is non-random and have provided a basis for investigating the consequences of their structure for dynamics (8, 6, 9), for an ecosystem's robustness to extinctions (10), and for the quantity and quality of services they provide (11, 12).

The simplest mathematical framework for food web structure dates back to the influential argument on stability and complexity, and it relied on the representation of connections between species based on random graphs (13). This model took into account only the species richness S and connectance C (fraction of realized feeding connections) of the web. The first nonrandom representation was given by the cascade model (5), which ordered species along a single dimension.

The biological basis for this ordering remains an open problem, but possibilities include body mass, trophic level, and metabolic rates (14, 9). Each species has a position in this hierarchy that determines its feeding relations, with prey chosen randomly only from the species whose ranking is lower than that of the predator. This rule makes all networks generated by this model acyclic, limiting its application to empirical food webs without cannibalism or feeding cycles. The niche model was proposed next (6, 15), in part to overcome this limitation. It retains the ordering of species in one dimension but adds the notion of a niche range, an interval that contains all the prey of a given predator. Although feeding cycles can now be generated, the resulting networks are, by construction, also interval, a property that is not

fully compatible with patterns in empirical food webs (7, 16).

Intervality has played an important role in the literature of food web models, because it is closely related to the number of dimensions needed to represent niches in a community (17, 7, 16). Technically, this property means that there exists a suitable ordering of the species for which all the prey of each predator are consecutive, with no gaps. In Fig. 1, matrix N , this property is apparent when the network is translated into a matrix representation; consecutive prey form an uninterrupted sequence of entries in each column. Although, for interval graphs, a single dimension should be sufficient, recent analyses indicate that food webs are only close to interval (16). As we show here, close to interval does not mean that a model assuming perfect intervality on a single axis can generate all the links in empirical food webs. A third and more recent model, the “nested hierarchy” (7), does not rely on niches in a one-dimensional space, but focuses instead on groups of species and considers implicitly phylogenetic constraints and adaptation (7). Closely related predators tend to share their prey with occasional departures from this phylogenetic constraint, as the result of adaptation to new environments and new prey (7). We focus here on these three static models of food web structure as the simplest and most used formulations; other models have been proposed that include more sophisticated construction rules, including dynamics and diet optimization, speciation, extinction, evolution (18–20), and adaptation (21).

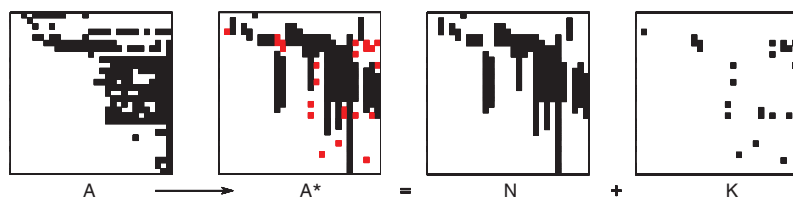


Fig. 1. Decomposition of a food web into two subwebs. For a given food web, we can write an adjacency matrix A . In this matrix, each coefficient represents the presence (1, black) or lack (0, white) of interaction between predator species (columns) and prey species (rows). We seek an ordering of the species that minimizes the number of irreducible connections, the links that are incompatible with the assumptions of a given model, in this case, the niche model. This yields the adjacency matrix A^* . The compatible connections of each predator i do fall into a segment (interval) such that the segment starts either before or on the i th species (hierarchy). The matrix N is formed by all the connections compatible with the niche model, and the matrix K contains all the irreducible connections.

¹Department of Ecology and Evolutionary Biology, University of Michigan, Natural Science Building, 830 North University, Ann Arbor, MI 48109, USA. ²National Center for Ecological Analysis and Synthesis, 735 State Street, Suite 300, Santa Barbara, CA 93101, USA. ³Community and Conservation Ecology Group, Center for Ecological and Evolutionary Studies, University of Groningen, Post Office Box 14, 9750 AA Haren, Netherlands. ⁴Santa Fe Institute, 1399 Hyde Park Road, Santa Fe, NM 87501, USA.

*To whom correspondence should be addressed. E-mail: allesina@nceas.ucsb.edu

The models have been previously compared with empirical data by simulating an ensemble of networks and by measuring a large set of summary statistics, such as the number of basal, intermediate, and top species; the average path length; the fraction of cannibalistic species; the degree of omnivory; and so on (6, 22, 23), for these networks. The performance of the model is inversely proportional to the distance between the simulated values and their empirical counterparts. The comparison of models based on this approach has several limitations. First, network properties are not independent. Second, the notion of distance requires knowledge of the natural variance of the different measures. In the absence of this information, the distribution of the models themselves has been used (6). Third, some models perform better for some indices and worse for others, which makes definitive comparisons elusive (22, 23), despite the increase in the number of network properties that have been considered. Possibly, the most striking caveat of the use of summary statistics is that it cannot tell us whether or not a model is able to fully replicate empirical networks.

We propose here a different approach based on likelihoods and, therefore, on the topology of the networks as a whole. That is, on the entire set of links that specify who consumes whom in the ecosystem, rather than on a collection of summary descriptors of structure. The likelihood that a model generates the observed data provides a single quantity that allows direct comparison between alternative models. We derive the likelihood for the cascade, niche, and nested-hierarchy models [(24), sections S1 to S3] and compare them.

Our starting point is that, strictly speaking, all the models have a likelihood of zero because they all fail to reproduce a subset of the links in the empirical webs. Thus, we arrive at a major limitation of current models: they are not general. For any ordering of the species, there are links that do not fulfill their assumptions. We refer to those links as irreproducible connections. Although this limitation has been known for the cascade and niche models (6, 7) it has not been addressed

before for the nested hierarchy. We show that this model also fails to replicate the empirical data: Most of the irreproducible links involve either cannibalism [a feeding relationship underrepresented by this model (7)] or lower-level species preying on higher level species [(24), section S3].

We therefore propose an additional step that consists of decomposing the original food web into two parts, the first composed of the links that are compatible with the specific model of interest and the second of those that the model cannot reproduce. Because the number of irreproducible connections depends on the ordering of the species in the trophic hierarchy [(24), sections S1 to S4], we used a genetic algorithm to find the ordering that minimizes this number. The process is sketched in Fig. 1 for the niche model. This then allows us effectively to formulate and compute a nontrivial likelihood for empirical webs. Each food web can be represented using a matrix (Fig. 1): We split the data into two matrices we call N and K for the reproducible and irreproducible connections, respectively. We then computed the probability of obtaining the matrix N using the model of interest and the probability of obtaining K using a random graph. The product of these two numbers gives us a total likelihood for the model. Although one could devise other ways to approach the problem of computing a likelihood, different from our decomposition, this would require specific assumptions about measurement errors [(24), section S1].

The number of irreproducible connections for each model and data set, together with the total likelihood, is shown in Table 1. The niche model has better likelihoods for all the considered food webs. However, the number of irreproducible connections for the niche model is much higher than that for the cascade and nested-hierarchy models. Thus, the niche model can reproduce a smaller subset of connections very well. This provides support for the central idea of this model that predators tend to consume prey that share common characteristics. However, the large number of irreproducible links indicates that one

single dimension is not sufficient to describe the similarity between prey animals or plants, a limitation that was raised before (7, 16).

To produce a general model that is able to generate the entire network, we then start from the niche model, as it provides a better baseline likelihood, and propose a simple way to address the multidimensionality of niche ranges. Predators can choose their prey according to several traits, such as prey body mass, movement, time of the day when foraging, color, presence or absence of antipredator behavior, and so on. A simple hypothetical example of the consequences of using a single trait to recover, from food web links, the range of predators' preference is illustrated in Fig. 2. When more than one trait underlies prey choice, the use of a single trait leads both to discontinuous ranges that contain gaps and to effective ranges that are smaller than the real ones. We therefore recover from network data only a minimum range and not its actual extent [(24), section S5].

A simple way to consider multidimensional niches [(24), sections S4 to S6] is to extend the niche model by including gaps into the diets of predators. In this minimum potential niche model, species are still ordered in a one-dimensional space, but each predator chooses a potential range (Fig. 2C). The two species at the extremes of the range are always prey (Fig. 2D, in black), and therefore, they delimit the extent of the minimum potential range. The other species contained in the range will be prey with probability $(1 - f)$, where f is the probability of a "forbidden link." Forbidden links have been introduced in the study of mutualistic networks to describe plant-animal interactions that are precluded by biological constraints, such as the short tongues of certain bees unable to efficiently pollinate long-corolla flowers (25–27). In our model, forbidden links implicitly take into account the existence of traits that are not explicitly considered when species and their niches are represented using a single dimension. The value of f specifies the fraction of nonrealized feeding interactions inside a potential range.

Table 1. Likelihood of the models for food web structure. For each model, we report the number of links (L), the number of irreproducible connections (I), the log-likelihood of obtaining such connections using random graphs [$\mathcal{L}(K)$] and the total log-likelihood for the model (Tot \mathcal{L}). $\mathcal{L}(N)$ can be obtained by difference. The Minimum potential niche model has no irreproducible con-

nections and results in better likelihoods for all cases. For this model, we show the probability of forbidden links (f). Note that the number of parameters is the same for all models, which allows a direct comparison of the likelihoods. In other cases, one can use criteria for model selection based on likelihoods, such as Akaike's information criterion.

Food web	Cascade					Niche			Nested hierarchy			Min. potential	
	S	L	I	$\mathcal{L}(K)$	Tot \mathcal{L}	I	$\mathcal{L}(K)$	Tot \mathcal{L}	I	$\mathcal{L}(K)$	Tot \mathcal{L}	Tot \mathcal{L}	f
Benguela	29	203	12	−62.91	−343.62	23	−105.46	−234.22	1	−7.73	−349.39	−213.52	0.170
Bridge	25	107	4	−24.19	−217.16	1	−7.44	−94.42	1	−7.44	−162.32	−92.18	0.013
Broom	85	223	4	−33.99	−857.42	36	−226.77	−737.56				−626.54	0.336
Chesapeake	31	68	1	−7.87	−199.59	10	−55.60	−166.84	3	−20.30	−200.15	−145.11	0.314
Coach	29	262	41	−163.85	−443.67	37	−151.75	−296.76	7	−40.49	−381.57	−296.10	0.240
Grass	61	97	0	0	−379.31	10	−69.18	−327.08	13	−86.52	−437.81	−294.94	0.243
Reef	50	556	59	−279.34	−1106.54	196	−687.11	−970.28	22	−126.03	−1053.50	−934.71	0.416
Skip	25	197	12	−59.32	−259.02	22	−95.24	−191.11	5	−29.12	−254.74	−169.67	0.142
St. Marks	48	221	3	−22.93	−576.69	72	−320.40	−546.48	18	−105.27	−634.04	−504.49	0.554
St. Martin	42	205	0	0	−472.58	52	−234.48	−421.53	10	−61.70	−531.55	−388.06	0.443

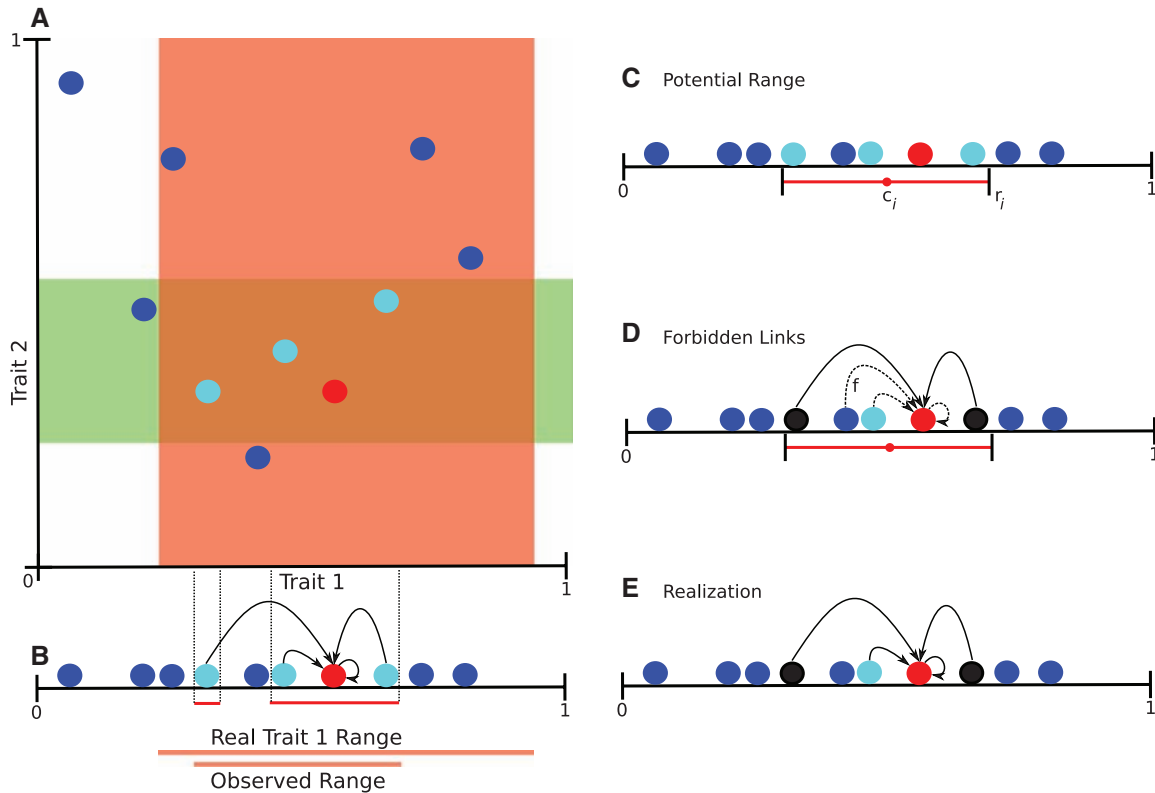


Fig. 2. Multidimensional niches and the minimum potential niche model. (A) A predator (in red) preys upon all the species falling in the overlap between two traits (red and cyan). If one tries to recover information on the range of trait 1 using the predator's diet, the observed range not only is smaller than the real one (B) but contains gaps. The minimal potential niche model starts

by assigning to each species a potential range, as in the niche model (C). This is done by considering that the first and the last species falling in the interval are prey (D) (black), and that the other species falling in the interval are prey with probability $1 - f$ [dashed line in (D)] where f provides a measure on nontrivial intervality [(24), section S4]. This model can reproduce discontinuous diets (E).

As a consequence, our model considers an effective niche range that is a subset of a fundamental (or potential) niche. A potential range, in order to include a forbidden link, must encompass at least three potential prey. Because of this, f represents a measure of nontrivial intervality in the network [(24), section S4].

The minimum potential niche model is a general model because it can reproduce all the links in the empirical food webs [e.g., (Fig. 2E)]. The derivation of the likelihood for this model follows as a straightforward modification of that for the niche model [(24), section S4]. The model requires three parameters: the number of species, S ; the density of potential connections, C_p ; and the probability of forbidden links, f . All three can be obtained from the empirical data. For all empirical data sets, the minimum potential niche model has the highest likelihood (Table 1).

Another simple solution to multidimensional niches and the related departure from intervality was previously proposed in a complementary approach known as the generalized niche model (GNM) (16). Instead of gaps within intervals, the GNM introduces "satellite prey" outside niche ranges. Despite the apparent similarity to the minimum potential niche model, the implementation of this approach appears problematic, and the model itself is unable to reproduce all links [(24), section S7].

In summary, the similarity between prey of a common predator on a one-dimensional niche space, which is the basis for the niche model, is well supported by empirical data. However, this property alone cannot account for all feeding relations in ecosystems, as previously noted (7, 16). We have proposed a simple way to take into account the multidimensionality of niches and to derive parameter values from the data. The proposed analysis, based on likelihoods, opens up the possibility of evaluating other fundamental assumptions of food web models, such as the existence of a hierarchy and the increased generality of predators along the niche axis. The derivation of a general model and its likelihood are also a critical first step toward evaluating the biological basis for the niche axis. It has been proposed that this axis could be mapped onto body mass, trophic levels, degree of specialization, and other characteristics of species (14, 28–30). The likelihood approach can be used for the quantitative testing of these hypotheses. Finally, this work sets a benchmark that can now be challenged by other, better models, for food web structure. The decomposition into compatible and incompatible links provides a natural starting point for improving particular models. There will always be types of models too complex for comparisons based on likelihoods, such as those that incorporate evolutionary processes explicitly

(18–21). However, simple models provide an opportunity to investigate which of the biological indices previously used for model comparisons better reflects the likelihood of a model.

References and Notes

1. S. L. Pimm, *Food Webs* (Chapman & Hall, New York, 1982).
2. J. A. Dunne, in *Ecological Networks: Linking Structure to Dynamics in Food Webs* (Oxford Univ. Press, Oxford, 2006), chap. 2.
3. J. M. Montoya, S. L. Pimm, R. V. Sole, *Nature* **442**, 259 (2006).
4. S. A. Levin, *Ecosystems* **1**, 431 (1998).
5. J. E. Cohen, C. M. Newman, *Proc. R. Soc. London Ser. B* **224**, 421 (1985).
6. R. J. Williams, N. D. Martinez, *Nature* **404**, 180 (2000).
7. M.-F. Cattin, L.-F. Bersier, C. Banasek-Richter, R. Baltensperger, J. P. Gabriel, *Nature* **427**, 835 (2004).
8. S. L. Pimm, J. H. Lawton, J. E. Cohen, *Nature* **350**, 669 (1991).
9. U. Brose, R. J. Williams, N. D. Martinez, *Ecol. Lett.* **9**, 1228 (2006).
10. J. A. Dunne, R. J. Williams, N. D. Martinez, *Ecol. Lett.* **5**, 558 (2002).
11. D. E. Schindler, S. R. Carpenter, J. J. Cole, J. F. Kitchell, M. L. Pace, *Science* **277**, 248 (1997).
12. J. M. Montoya, M. A. Rodríguez, B. A. Hawkins, *Ecol. Lett.* **6**, 587 (2003).
13. R. M. May, *Nature* **238**, 413 (1972).
14. G. Woodward *et al.*, *Trends Ecol. Evol.* **20**, 402 (2005).
15. R. J. Williams, N. D. Martinez, *Eur. Phys. J. B* **38**, 297 (2004).
16. D. B. Stouffer, J. Camacho, L. A. N. Amaral, *Proc. Natl. Acad. Sci. U.S.A.* **103**, 19015 (2006).
17. J. E. Cohen, *Proc. Natl. Acad. Sci. U.S.A.* **74**, 4533 (1977).
18. G. Caldarelli, P. G. Higgs, A. J. McKane, *J. Theor. Biol.* **193**, 345 (1998).

19. N. Loeuille, M. Loreau, *Proc. Natl. Acad. Sci. U.S.A.* **102**, 5761 (2005).
20. A. G. Rossberg, H. Matsuda, T. Amemiya, K. Itoh, *Ecol. Complex.* **2**, 312 (2005).
21. A. G. Rossberg, H. Matsuda, T. Amemiya, K. Itoh, *J. Theor. Biol.* **241**, 552 (2006).
22. N. D. Martinez, L. J. Cushing, in *Ecological Networks: Linking Structure to Dynamics in Food Webs* (Oxford Univ. Press, Oxford, 2006), Box A, p. 87.
23. L.-F. Bersier, M.-F. Cattin, C. Banasek-Richter, R. Baltensperger, J.-P. Gabriel, in *Ecological Networks: Linking Structure to Dynamics in Food Webs* (Oxford Univ. Press, Oxford, 2006), Box B, p. 91.
24. Details of the model are given in *Science* Online.
25. P. Jordano, J. Bascompte, J. M. Olesen, *Ecol. Lett.* **6**, 69 (2003).
26. D. P. Vazquez, *Oikos* **108**, 421 (2005).
27. L. Santamaría, M. A. Rodríguez-Gironés, *PLoS Biol.* **5**, e31 (2007).
28. M. G. Neubert, S. C. Blumenshine, T. Jonsson, B. Rashleigh, *Oecologia* **123**, 241 (2000).
29. C. A. Layman, K. O. Winemiller, D. A. Arrington, D. B. Jepsen, *Ecology* **86**, 2530 (2005).
30. T. Jonsson, J. E. Cohen, S. R. Carpenter, *Adv. Ecol. Res.* **36**, 1 (2005).
31. We thank The Center for the Study of Complex Systems at the University of Michigan for computational resources.

Andy Dobson and two anonymous reviewers for insightful comments, and Café Ambrosia for a comfortable meeting place. This work was supported by a Centennial Fellowship of the James S. McDonnell Foundation to M.P.

Supporting Online Material

www.sciencemag.org/cgi/content/full/320/5876/658/DC1
Materials and Methods
Figs. S1 to S13
Tables S1 to S8
References

8 February 2008; accepted 27 March 2008
10.1126/science.1156269

ROS-Generating Mitochondrial DNA Mutations Can Regulate Tumor Cell Metastasis

Kaori Ishikawa,^{1,2,3*} Keizo Takenaga,^{4,5*} Miho Akimoto,⁵ Nobuko Koshikawa,⁴ Aya Yamaguchi,¹ Hirotake Imanishi,¹ Kazuto Nakada,^{1,2} Yoshio Honma,⁵ Jun-Ichi Hayashi^{1†}

Mutations in mitochondrial DNA (mtDNA) occur at high frequency in human tumors, but whether these mutations alter tumor cell behavior has been unclear. We used cytoplasmic hybrid (cybrid) technology to replace the endogenous mtDNA in a mouse tumor cell line that was poorly metastatic with mtDNA from a cell line that was highly metastatic, and vice versa. Using assays of metastasis in mice, we found that the recipient tumor cells acquired the metastatic potential of the transferred mtDNA. The mtDNA conferring high metastatic potential contained G13997A and 13885insC mutations in the gene encoding NADH (reduced form of nicotinamide adenine dinucleotide) dehydrogenase subunit 6 (*ND6*). These mutations produced a deficiency in respiratory complex I activity and were associated with overproduction of reactive oxygen species (ROS). Pretreatment of the highly metastatic tumor cells with ROS scavengers suppressed their metastatic potential in mice. These results indicate that mtDNA mutations can contribute to tumor progression by enhancing the metastatic potential of tumor cells.

Because most chemical carcinogens bind preferentially to mitochondrial DNA (mtDNA) rather than to nuclear DNA (1–3), mtDNA is considered to be their major cellular target. It has been hypothesized that the resultant somatic mutations in mtDNA play a causal role in oncogenic transformation (3). Many subsequent studies have supported the idea of preferential accumulation of somatic mutations in tumor mtDNAs (4–9) and their contribution to tumor growth (10, 11). However, the apparent high frequency of mtDNA mutations in tumors could be due either to their stochastic accumulation (12, 13) or to laboratory errors (14). Moreover, if mtDNA mutations induce oncogenic transformation, all the offspring of a mother carrying such mutations should

develop tumors due to the maternal inheritance of mtDNA (15, 16), but no bias toward maternal inheritance of tumor development has been reported. Nonetheless, it remains possible that mtDNA mutations are involved at a later stage of tumorigenesis, for example, in the development of metastatic potential. Recent studies demonstrated that dysfunction of the tricarboxylic acid cycle (TCA cycle) caused by mutations in nuclear DNA controls tumor phenotypes by the induction of a pseudo-hypoxic pathway under normoxic conditions (17–19). However, there has been no evidence of the involvement of mtDNA mutations in the development of metastatic potential or in the regulation of the pseudo-hypoxic pathway because of the difficulty of excluding possible involvement of nuclear DNA mutations in these processes (20).

We have examined the role of pathogenic mtDNA mutations in the development of tumor cell metastasis by studying two mouse tumor cell lines with different metastatic potentials (low metastatic P29 and high metastatic A11 cells) that originated from Lewis lung carcinoma (table S1) (21–23). We compared mitochondrial respiratory function by estimating the activities of respiratory complexes and found that P29 cells had normal activities, whereas A11 cells showed reduced ac-

tivity of complex I (NADH dehydrogenase) (Fig. 1A). Complex I defects were also observed in high metastatic fibrosarcoma B82M cells but not in high metastatic colon adenocarcinoma LuM1 cells (Fig. 1A), which suggests that metastatic tumors are not always associated with complex I defects.

Because complex I consists of subunits encoded by both nuclear DNA and mtDNA (24), it was necessary to determine which genome, nuclear or mitochondrial, was responsible for the complex I defects and whether the complex I defects were responsible for the high metastatic potential. We addressed these issues by complete reciprocal exchange of mtDNAs between P29 and A11 cells by means of cell fusion to isolate transmtochondrial cybrids (fig. S1A and table S2) and examined whether complex I defects and metastatic potentials were cotransferred with the mtDNA. The results showed that complex I activity decreased in the cybrids with A11 mtDNA, whereas those with P29 mtDNA showed normal activity, irrespective of whether their nuclear DNAs were derived from P29 or A11 cells (Fig. 1B). Thus, complex I defects in the cybrids with A11 mtDNA appear to result from pathogenic mutations in their mtDNA, not in their nuclear DNA. We then examined the metastatic potential of the cybrids by inoculating them into a tail vein (to test “experimental” metastasis) and under the skin (to test “spontaneous” metastasis) of C57BL/6 mice and counting the number of nodules formed in the lung. Cybrids with A11 mtDNA acquired high metastatic potential, whereas cybrids with P29 mtDNA lost metastatic potential (table S2). These observations suggest that complex I defects and high metastatic potential are transferred simultaneously with the transfer of mtDNA from the A11 cells, whereas normal complex I activity and low metastatic potential are transferred simultaneously with the transfer of mtDNA from P29 cells. The mtDNA of A11 cells is therefore likely to harbor a mutation(s) responsible for complex I defects and metastasis.

We next examined whether these findings could be generalized to additional tumor cell lines. In these experiments, we transferred mtDNA from A11 cells into fibrosarcoma B82 cells with low metastatic potential and normal complex I activity, resulting in isolation of B82mtA11 cybrids (table S2). Conversely, we transferred mtDNA from B82M cells, which are derived from B82 cells but express high metastatic potential and com-

¹Graduate School of Life and Environmental Sciences, University of Tsukuba, 1-1-1 Tennodai, Tsukuba, Ibaraki 305-8572, Japan.

²Tsukuba Advanced Research Alliance Center, University of Tsukuba, 1-1-1 Tennodai, Tsukuba, Ibaraki 305-8572, Japan.

³Japan Society for the Promotion of Science (JSPS), 8 Ichiban-cho, Chiyoda-ku, Tokyo 102-8472, Japan.

⁴Division of Chemotherapy, Chiba Cancer Center Research Institute, 666-2 Nitona, Chuo-ku, Chiba 260-8717, Japan. ⁵Shimane University Faculty of Medicine, 89-1 Enya-cho, Izumo, Shimane 693-8501, Japan.

*These authors contributed equally to this work.

†To whom correspondence should be addressed. E-mail: jih45@sakura.cc.tsukuba.ac.jp